Metabolic Engineering 38 (2016) 285–292

Contents lists available at ScienceDirect

Metabolic Engineering

journal homepage: www.elsevier.com/locate/ymben

Original Research Article

Engineering nonphosphorylative metabolism to synthesize mesaconate from lignocellulosic sugars in *Escherichia coli*

Wenqin Bai[a,b,c], Yi-Shu Tai[a], Jingyu Wang[a], Jilong Wang[a], Pooja Jambunathan[a], Kevin J. Fox[a], Kechun Zhang[a,*]

[a] *Department of Chemical Engineering and Materials Science, University of Minnesota, Minneapolis, MN 55455, USA*
[b] *Tianjin Institute of Industrial Biotechnology, Chinese Academy of Sciences, Tianjin 300308, China*
[c] *College of Life Science, Shanxi Normal University, Linfen 041004, China*

ARTICLE INFO

Keywords:
Escherichia coli
Nonphosphorylative metabolism
Dicarboxylic acid
Mesaconate
Pentose

ABSTRACT

Dicarboxylic acids are attractive biosynthetic targets due to their broad applications and their challenging manufacturing process from fossil fuel feedstock. Mesaconate is a branched, unsaturated dicarboxylic acid that can be used as a co-monomer to produce hydrogels and fire-retardant materials. In this study, we engineered nonphosphorylative metabolism to produce mesaconate from D-xylose and L-arabinose. This nonphosphorylative metabolism is orthogonal to the intrinsic pentose metabolism in *Escherichia coli* and has fewer enzymatic steps and a higher theoretical yield to TCA cycle intermediates than the pentose phosphate pathway. Here mesaconate production was enabled from the D-xylose pathway and the L-arabinose pathway. To enhance the transportation of D-xylose and L-arabinose, pentose transporters were examined. We identified the pentose/proton symporter, AraE, as the most effective transporter for both D-xylose and L-arabinose in mesaconate production process. Further production optimization was achieved by operon screening and metabolic engineering. These efforts led to the engineered strains that produced 12.5 g/l and 13.2 g/l mesaconate after 48 h from 20 g/l of D-xylose and L-arabinose, respectively. Finally, the engineered strain overexpressing both L-arabinose and D-xylose operons produced 14.7 g/l mesaconate from a 1:1 D-xylose and L-arabinose mixture with a yield of 85% of the theoretical maximum. (0.87 g/g). This work demonstrates an effective system that converts pentoses into a value-added chemical, mesaconate, with promising titer, rate, and yield.

1. Introduction

Dicarboxylic acids have extensive applications in the polymer industry for preparation of copolymers such as polyesters and polyamide (Bechthold et al., 2008). Moreover, dicarboxylic acids can be hydrogenated to form the corresponding diols. For example, succinic acid can be hydrogenated to produce 1,4-butanediol (Hong et al., 2013). However, the manufacture processes of most fossil feedstock-derived dicarboxylic acid are not only energy intensive and unsustainable, but also environmentally unfriendly (Adom et al., 2014). For example, nitric acid oxidation is widely used to produce a dicarboxylic acid, adipic acid, and nitrous oxide (N_2O) emitted during the process is considered to cause global warming and ozone depletion (Sato et al., 1998). Due to these intrinsic disadvantages of fossil feedstock-derived processes, dicarboxylic acids are attractive targets for biosynthesis from bio-based feedstock (Lopez-Garzon and Straathof, 2014).

Mesaconate is a branched, unsaturated dicarboxylic acid that was found in *Clostridium tetanomorphum* (Blair and Barker, 1966) and *Burkholderiaxenovorans* (Kronen et al., 2015). It is an intermediate in the glutamate degradation pathway and can be further converted into pyruvate and acetyl-CoA. Mesaconate can be co-polymerized with acrylamide and crosslinked with ethylene glycol dimethacrylate or 1,4-butanediol dimethacrylate to form hydrogels (Uzum and Karadag, 2005). These hydrogels have both high water absorbency and equilibrium water content which show biomedical potential. Dialkyl esters of mesaconate can undergo Diels-Alder reactions to give bicyclic compounds (White and Sheldon, 1981) and diallyl esters of mesaconate can be used to produce flame retardant materials (Gillham and Sherr, 1969). Moreover, mesaconate can also be reduced by an oxygen-regulated periplasmic reductase (Mfr) from *Campylobacter jejuni*to form 2-methylsuccinate (Guccione et al., 2010). Overall, mesaconate is a versatile platform chemical that has broad applications. Two pathways have been reported for mesaconate biosynthesis. The first one utilizes the intermediate mesaconyl-CoA generated from the ethylma-

* Corresponding author.
E-mail address: kzhang@umn.edu (K. Zhang).

http://dx.doi.org/10.1016/j.ymben.2016.09.007
Received 13 June 2016; Received in revised form 20 September 2016; Accepted 29 September 2016
Available online 30 September 2016
1096-7176/ © 2016 International Metabolic Engineering Society. Published by Elsevier Inc. All rights reserved.

lonyl–CoA pathway and expresses a heterologous thioesterase to convert it to mesaconate. The pathway was engineered in strain *Methylobacteriumextorquens* AM1 and enabled production of 443 mg/l mesaconate from methanol after optimization (Sonntag et al., 2014, 2015). The other pathway is a natural pathway which converts glutamate into mesaconate by glutamate mutase and 3-methylaspartate ammonia lyase (MAL). The pathway has been identified in various *Clostridium* strains (Buckel and Barker, 1974) and has been heterologously reconstructed in the industrial workhorse *Escherichia coli* (Wang and Zhang, 2015). The engineered *E. coli* strain enabled the production of 6.96 g/l of mesaconate from glucose after optimization (Wang and Zhang, 2015).

Lignocellulosic waste is an attractive biomass to use in second generation biorefineries due to its abundant availability and low cost. The simultaneous consumption of all biomass sugars is a major challenge in engineering *E. coli* for fermentation of lignocellulose-derived sugars (Jojima et al., 2010). Pentoses like D-xylose and L-arabinose, which can make up to 30% of plant biomass, are the most abundant sugars in hemicellulose (Weber et al., 2010). Therefore, efficient utilization of pentoses is critical to an economically viable biosynthetic process. Wild type *E. coli* can use pentoses as the carbon source (Feldmann et al., 1992). However, the utilization of D-xylose or L-arabinose is normally inhibited in the presence of glucose due to carbon catabolite repression (CCR) (Goerke and Stulke, 2008) since glucose can effectively block the expression of pentose transporters and key enzymes needed for pentose metabolism. Previous research mainly focused on engineering phosphotransferase system (PTS) (Dien et al., 2002) or a constitutively active CRP allele (Cirino et al., 2006) to alleviate CCR, but usually did not result in an effective strain. For example, an *E. coli* strain with a *ptsG* mutant could use D-xylose and glucose simultaneously to produce lactic acid, but it could not completely consume D-xylose and the yields of lactic acid decreased with increasing glucose feeding (Dien et al., 2002). Recent studies found that L-arabinose can repress D-xylose utilization due to L-arabinose-bound AraC (Desai and Rao, 2010; Jarmander et al., 2014) and D-xylose can also repress the expression of the L-arabinose metabolic genes due to XylR (Koirala et al., 2016). The mutual repression of pentose utilization systems complicates simultaneous mixed-sugar utilization. Moreover, the intrinsic metabolism for pentoses (pentose phosphate pathway and glycolysis) requires at least 10 enzymatic steps to reach the TCA cycle and has a low theoretical yield at 83 mol% to a key TCA cycle intermediate 2-ketoglutarate (2-KG). A promising alternative metabolism for pentoses has been found in some archaea or extremophiles strains (Weimberg, 1961). This metabolism is nonphosphorylative and can effectively convert pentoses such as D-xylose and L-arabinose into 2-KG with only five enzymatic steps and a 100 mol% theoretical yield from pentoses to 2-KG (Tai et al., 2016). Moreover, this nonphosphorylative metabolism is orthogonal to the intrinsic pentose metabolism and thus may serve as an attractive way to alleviate the CCR and reciprocal repression on the key enzymes needed for pentose metabolism.

In this work, we first demonstrate mesaconate production from D-xylose and L-arabinose based on the nonphosphorylative biosynthetic platform. To enhance pentose uptake rates during the fermentation process, various pentose transporters were examined based on the improvement of mesaconate production titers. Different nonphosphorylative operons were also screened for D-xylose and L-arabinose, respectively. To further optimize mesaconate production from these pentoses, metabolic engineering strategies were applied by knocking out a competing pathway and enlarging the intracellular glutamate pool. The final engineered strains enabled 12.5 g/l and 13.2 g/l mesaconate production from D-xylose and L-arabinose after 48 h, respectively. Finally, we examined the co-utilization of glucose, D-xylose, and L-arabinose to biosynthesize mesaconate. The strain overexpressing D-xylose and L-arabinose operons simultaneously could produce 14.7 g/l mesaconate after 48 h with a yield of 0.74 g mesaconate/g of combined D-xylose and L-arabinose. This represents 85% of the theoretical yield (0.87 g/g sugar). This study presents the systematic metabolic engineering efforts on optimizing mesaconate production titer, rate, and yield from biomass sugars D-xylose and L-arabinose and enables a novel and promising mesaconate biosynthetic process.

2. Materials and methods

2.1. Bacterial and growth conditions

E. coli strains used in this study are listed in Table S1 in Supplementary materials. *E. coli* strain XL10-Gold (Stratagene) was used for cloning. Other strains were derived from the wild type *E. coli* K-12 strain BW25113. The P1 phage of *sucA* was obtained from the Keio collection (Baba et al., 2006). Phage was used to transfect the corresponding strains for construction of targeted knockout strains (Miller, 1972). All the knockout strains were then transformed with pCP20 plasmid to remove the kanamycin marker. The correct knockouts were verified by colony PCR. Unless otherwise stated, these *E. coli* strains were grown in test tubes at 37 °C in 2×YT rich medium (16 g/l tryptone, 10 g/l yeast extract, and 5 g/l NaCl) supplemented with appropriate antibiotics (100 mg/l ampicillin, 50 mg/l kanamycin, and 100 mg/l spectinomycin). Chemicals used in the study were purchased from Sigma-Aldrich unless otherwise specified.

2.2. Plasmids construction

All plasmids used in the study are listed in Table S1. All primers used in this study were ordered from Eurofins MWG Operon and are listed in Table S2. PCR reactions were carried out with Q5 High-Fidelity DNA polymerase (New England Biolabs) according to the manufacturer's instructions. FastDigest restriction enzymes were purchased from Thermo Scientific. Sequences of all the plasmids constructed were verified by restriction mappings and DNA sequencing.

The recombinant plasmid pM-3 was constructed as follows: gene *DR64_8450* was amplified from plasmid pM-1 using primer pairs DR64_8450-F and DR64_8450-R. The linearized pZA vector containing genes *xylB-xylC-xylD* was obtained by digesting plasmid pM-2 with restriction enzymes HindIII and BlpI. The amplified *DR64_8450* fragment was then ligated onto the linearized pZA vector using NEBuiderHiFi DNA Assembly Master Mix (*New England Biolabs*). The recombinant plasmid pM-10 was constructed as follows: *xylA* gene was amplified from plasmid pM-9 by PCR using xylA-F and xylA-R as primers. Gene fragment of *glmE* was amplified from plasmid pM-7 by PCR using glmE-F and glmE-R as primers. The amplified *xylA* PCR product was digested with SdaI and XbaI, *glmE* PCR product was digested with SphI and SdaI, and then they were ligated into the linearized vector generated by digesting plasmid pM-7 with SphI and XbaI. The recombinant plasmid pM-11 was constructed as follows: *xylE* gene was amplified from *E. coli* BW25113 genomic DNA by PCR using xylE-F and xylE-R as primers. PCR product of *xylE* was digested by SphI and BamHI, and then ligated into the linearized vector generated by digesting pM-8 with the same enzymes. The construction of the recombinant plasmid pM-12 is similar to that of pM-11, but PCR product of *araE* was amplified using araE-F and araE-R as primers and was digested with SphI and BglII. The recombinant plasmid pM-15 was constructed as follows: *xylFGH*gene was amplified from *E. coli* BW25113 genomic DNA by PCR using xylFGH-F1 and xylFGH-R1 as primers. Then the PCR product was digested with KpnI and HindIII, and then ligated into the plasmid pM-13 digested by the same set of restriction enzymes. Then the plasmid pM-14 was obtained. Next, *xylFGH* fragment containing both promoter and terminator regions was amplified from plasmid pM-14 by PCR using xylFGH-F2 and xylFGH-R2 as primers. The fragment containing *btuB* gene was amplified from pM-8 by PCR using btuB-F and btuB-R. Then the two PCR fragments and the linearized pM-8 (digested KpnI and HindIII)

were purified and ligated into the plasmid pM-8 between XhoI and PstI sites using NEBuiderHiFi DNA Assembly Master Mix. The construction of the recombinant plasmids pM-16 and pM-17 was similar to that of pM-15, but the two primer sets used were AraFGH-F1 and AraFGH-R1, and AraFGH-F2 and AraFGH-R2. The recombinant plasmid pM-19 was constructed as follows: *gdhA* was amplified from *E. coli* BW25113 genomic DNA by PCR using gdhA-F1 and gdhA-R1 as primers. Then the PCR product was digested by *Kpn*I and *Hin*dIII, and then ligated into plasmid pM-13 digested by the same restriction enzymes to obtain plasmid pM-18. Next, the *gdhA* fragment containing promoter and terminator regions was amplified from pM-18 by PCR using gdhA-F2 and gdhA-R2 as primers. The fragment containing *btuB* gene was amplified from pM-8 by PCR using btuB-F and btuB-R as primers. Then the two PCR fragments (*gdhA* and *btuB*) were purified and ligated into the linearized vector created by digesting plasmid pM-11 with XhoI and PstI using NEBuiderHiFi DNA Assembly Master Mix. The construction of the recombinant plasmid pM-20 was similar to that of pM-19, but the PCR products were ligated into the plasmid pM-12 instead of pM-11 between XhoI and PstI sites. The recombinant plasmid pM-21 was constructed as follows: L-arabinose operon containing the promoter and terminator was amplified from the plasmid pM-3 using araABCD-F and araABCD-R as primers. Xylose operon containing the promoter and terminator was amplified from the plasmid pM-4 using xylABCD-F and xylABCD-R as primers. pZAlac linear vector was amplified from plasmid pM-3 using pZA-F and pZA-R as primers. After purification, the three PCR fragments were ligated to form a recombinant plasmid pM-21 by using NEBuiderHiFi DNA Assembly Master Mix.

2.3. Shake flask fermentation

125-ml conical flasks with 0.5 g $CaCO_3$ (used to buffer the pH of media) were autoclaved and dried to perform all small-scale fermentations. The flasks were filled with 5 ml fermentation medium (M9 minimal media supplemented with 5 g/l yeast extract, 20*g*/l glucose, 20 g/l D-xylose (or L-arabinose), 5 μM coenzyme B12, 100 mg/l ampicillin, 50 mg/l kanamycin, and 100 mg/l spectinomycin). For *sucA* deletion strains MX2 and MA2, 5 mM succinic acid was supplemented. To start fermentation, 200 μl of overnight cultures incubated in 2×YT medium were transferred into the flasks. After adding 0.5 mM isopropyl-β-D-thiogalactoside (IPTG), the flasks were put into a shaker at 250 rpm and 30 °C, and the fermentation was performed for 48 h. The fermentation products were analyzed by HPLC. Error bars indicated the SD of the results obtained from three independent experiments (n=3) by picking three different colonies for fermentation.

2.4. Metabolite analysis

Fermentation samples were analyzed using an Agilent 1260 Infinity HPLC system equipped with an Aminex HPX-87H column(Bio-Rad) and a refractive-index detector. The automated liquid sampler program and mobile phase gradient program were performed as manufacturer's instruction. The mobile phase is 0.01 N H_2SO_4 with a flow rate 0.6 ml/min. The column temperature and the RID detector temperature are 35 °C and 50 °C, respectively.

3. Results and discussion

3.1. Mesaconate production from nonphosphorylative metabolism

To efficiently use pentoses (D-xylose and L-arabinose) as feedstocks for mesaconate production, biosynthetic pathways were designed by expanding the nonphosphorylative metabolism (Fig. 1). In the D-xylose pathway, D-xylose is converted into 2-KG with five enzymatic steps enabled by D-xylose dehydrogenase (XDH), D-xylonolactonase (XL), D-xylonate dehydratase (XD), 2-keto-3-deoxy-D-xylonate dehydratase (KdxD), and 2-ketoglutarate semialdehyde dehydrogenase (KGSADH) (Brouns et al., 2006). Similarly, L-arabinose is transformed into 2-KG by L-arabinose dehydrogenase (ADH), L-arabinolactonase (AL), L-arabonate dehydratase (AD), 2-keto-3-deoxy-L-arabonate dehydratase (KdaD), and 2-ketoglutarate semialdehyde dehydrogenase (KGSADH). 2-KG produced from the nonphosphorylative metabolism is converted into glutamate by glutamate dehydrogenase. 3-methylaspartate is then produced from glutamate by glutamate mutase and then is converted into mesaconate by MAL..

Based on the pathway design, we constructed two strains, strain 1 and strain 2 (Table 1), to synthesize mesaconate from D-xylose and L-arabinose, respectively. In strain 1 (MX1, BW25113 Δ*xylA,* Δ*yihH,* Δ*yagE,* Δ*icd*), a D-xylose operon from *Burkholderiaxenovorans LB400* was overexpressed by a medium-copy plasmid (pZA-*DR64_8447-8448-8449-8450*) to produce 2,5-dioxopentanoate (DOP), and genes for DOP to mesaconate pathway were cloned into a high-copy plasmid (pZE-*MAL-MutL-mutS-glmE-xylA*$_{CC}$). Finally, the regeneration and reactivation enzymes for coenzyme B12 were expressed by a low-copy plasmid (pZS-*btuB-btuR-fpr-fldA*) to maintain the activity of the B12-dependent glutamate mutase. Strain 2 (MA1, BW25113 Δ*icd*) contains an L-arabinose operon from *Burkholderiamultivorans* on a medium-copy plasmid (pZA-*araC-araD-araA-araB*) and the same other two plasmids (pZE-*MAL-MutL-mutS-glmE-xylA*$_{CC}$ and pZS-*btuB-btuR-fpr-fldA*) as in strain 1. The two strains were then examined by fermentation for the production of mesaconate. After 48 h, strain 1 successfully produced 3.47 g/l mesaconate from 20 g/l of D-xylose and strain 2 produced 3.08 g/l of mesaconate from 20 g/l of L-arabinose. Glucose (20 g/l) was supplemented for cell growth, but did not contribute to mesaconate production due to the *icd* deletion. These preliminary results demonstrate an efficient conversion from the two pentoses, D-xylose and L-arabinose, to mesaconate via the nonphosphorylative metabolism.

3.2. Overexpression of pentose transporters to enhance substrate uptake

When glucose and D-xylose mixtures (strain 1) or glucose and L-arabinose mixtures (strain 2) were used for mesaconate production, we observed CCR (Desai and Rao, 2010; Stulke and Hillen, 1999) since glucose is the preferred substrate for *E. coli*. For strain 1, only 8.3 g/l of D-xylose was consumed after 48 h; for strain 2, only 9.3 g/l of L-arabinose was consumed, while glucose (20 g/l) was completely consumed in both experiments. Since this nonphosphorylative metabolism is not regulated by glucose, we believe that CCR can be alleviated by enhancing pentose transportation. Thus, various pentose transporters were tested in the engineered strains for their ability to facilitate pentose transportation.

There are two pentose transporter systems in *E. coli*. One system contains ATP-binding cassette (ABC) transporters (XylFGH and AraFGH) which have higher affinity but lower capacity. The other system contains pentose/proton symporters (XylE and AraE) which shows lower affinity but higher capacity (Daruwalla et al., 1981; Hasona et al., 2004). It is well known that the low-affinity symporters are promiscuous and can transport heterologous sugars (Shamanna and Sanderson, 1979; Song and Park, 1998). Therefore, we constructed three strains (strains 3, 4, and 5) for D-xylose fermentation. These three strains based on MX1 strain were all transformed with the plasmids containing D-xylose to mesaconate pathway, pZA-*DR64_8447-8448–8449–8450* and pZE-*MAL-MutL-mutS-glmE-xylA*$_{CC}$, and different pentose transporters were cloned into the pZS plasmid. XylE, XylFGH, and AraE were overexpressed in strain 3, strain 4, and strain 5, respectively. Due to the high-affinity nature of the ABC transporter, AraFGH was not used for the D-xylose pathway. The fermentation results (Fig. 2**A**) showed that strain 5 (AraE) enabled the highest mesaconate production titer, 6.59 g/l after 48 h, from D-xylose. The ABC transporter XylFGH (strain 4) produced only slightly higher titer

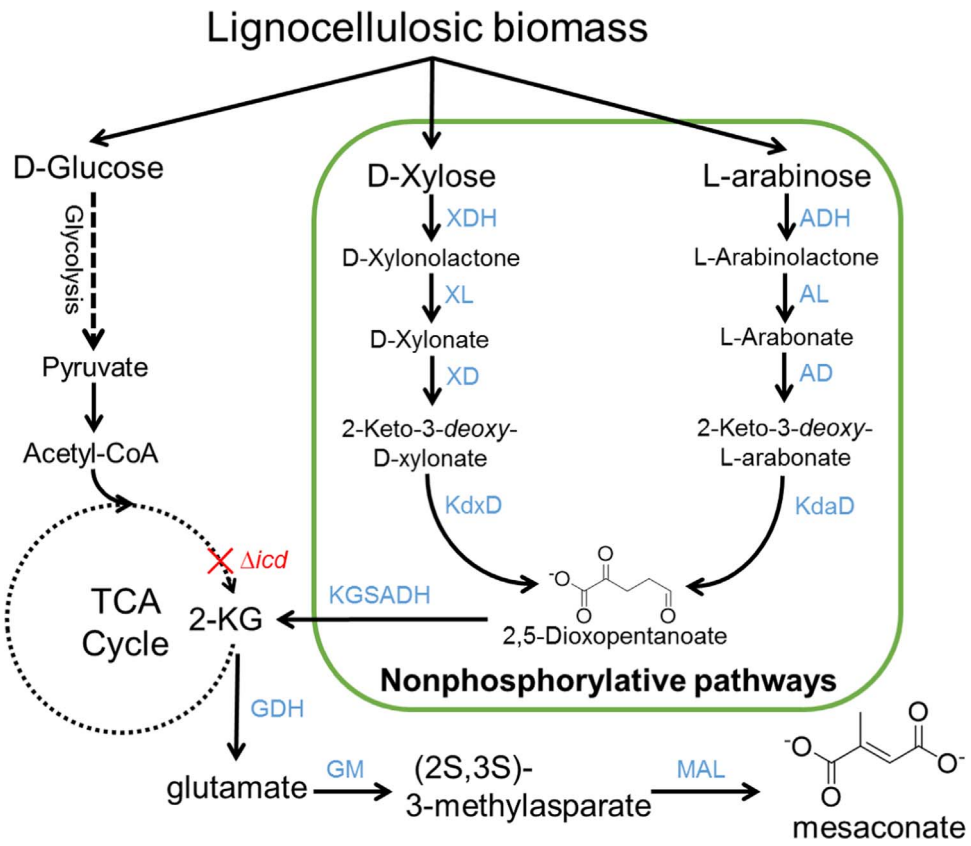

Fig. 1. Metabolic pathways from lignocellulosic sugars to mesaconate via nonphosphorylative metabolism. The pathway for D-xylose consists of D-xylose dehydrogenase (XDH), D-xylonolactonase (XL), D-xylonate dehydratase (XD), and 2-keto-3-deoxy-D-xylonate dehydratase (KdxD). The L-arabinose assimilation pathway is composed of L-arabinose dehydrogenase (ADH), L-arabinolactonase (AL), L-arabonate dehydratase (AD), and 2-keto-3-deoxy-L-arabonate dehydratase (KdaD). The produced DOP is then converted into 2-ketoglutarate (2-KG) by 2-ketoglutarate semialdehyde dehydrogenase (KGSADH). 2-KG is then transformed to mesaconate by glutamate dehydrogenase (GDH), glutamate mutase (GM), and 3-methylaspartate ammonia lyase (MAL).

Table 1
List of strains used in this study.

Strain no.	*E. coli* strain	Plasmid 1	Plasmid 2	Plasmid 3
1	MX1	pZE-*MAL-MutL-mutS-glmE-xylA*$_{CC}$	pZA-*DR64_8447-8448-8449-8450*	pZS-*btuB-btuR-fpr-fldA*
2	MA1	pZE-*MAL-MutL-mutS-glmE-xylA*$_{CC}$	pZA-*araC-araD-araA-araB*	pZS-*btuB-btuR-fpr-fldA*
3	MX1	pZE-*MAL-MutL-mutS-glmE-xylA*$_{CC}$	pZA-*DR64_8447-8448-8449-8450*	pZS-*btuB-btuR-fpr-fldA-xylE*
4	MX1	pZE-*MAL-MutL-mutS-glmE-xylA*$_{CC}$	pZA-*DR64_8447-8448-8449-8450*	pZS-*btuB-btuR-fpr-fldA-xylFGH*
5	MX1	pZE-*MAL-MutL-mutS-glmE-xylA*$_{CC}$	pZA-*DR64_8447-8448-8449-8450*	pZS-*btuB-btuR-fpr-fldA-araE*
6	MA1	pZE-*MAL-MutL-mutS-glmE-xylA*$_{CC}$	pZA-*araC-araD-araA-araB*	pZS-*btuB-btuR-fpr-fldA-araE*
7	MA1	pZE-*MAL-MutL-mutS-glmE-xylA*$_{CC}$	pZA-*araC-araD-araA-araB*	pZS-*btuB-btuR-fpr-fldA-araFGH*
8	MA1	pZE-*MAL-MutL-mutS-glmE-xylA*$_{CC}$	pZA-*araC-araD-araA-araB*	pZS-*btuB-btuR-fpr-fldA-xylE*
9	MX1	pZE-*MAL-MutL-mutS-glmE-xylA*$_{CC}$	pZA-*xylB-xylC-xylD-xylX*	pZS-*btuB-btuR-fpr-fldA-araE*
10	MX1	pZE-*MAL-MutL-mutS-glmE-xylA*$_{CC}$	pZA-*xylB-xylC-xylD-DR64_8450*	pZS-*btuB-btuR-fpr-fldA-araE*
11	MA1	pZE-*MAL-MutL-mutS-glmE-xylA*$_{CC}$	pZA-*Bamb_4925-4923-4922-4918*	pZS-*btuB-btuR-fpr-fldA-araE*
12	MA1	pZE-*MAL-MutL-mutS-glmE-xylA*$_{CC}$	pZA-*BTH_II1632-1630-1629-1625*	pZS-*btuB-btuR-fpr-fldA-araE*
13	MX2	pZE-*MAL-MutL-mutS-glmE-xylA*$_{CC}$	pZA-*xylB-xylC-xylD-DR64_8450*	pZS-*btuB-btuR-fpr-fldA-araE*
14	MX2	pZE-*MAL-MutL-mutS-glmE-xylA*$_{CC}$	pZA-*xylB-xylC-xylD-DR64_8450*	pZS-*gdhA-btuB-btuR-fpr-fldA-araE*
15	MA2	pZE-*MAL-MutL-mutS-glmE-xylA*$_{CC}$	pZA-*Bamb_4925-4923-4922-4918*	pZS-*btuB-btuR-fpr-fldA-araE*
16	MA2	pZE-*MAL-MutL-mutS-glmE-xylA*$_{CC}$	pZA-*Bamb_4925-4923-4922-4918*	pZS-*gdhA-btuB-btuR-fpr-fldA-araE*
17	MX2	pZE-*MAL-MutL-mutS-glmE-xylA*$_{CC}$	pZA-*Bamb_4925-4923-4922-4918-xylB-xylC-xylD-DR64_8450*	pZS-*gdhA-btuB-btuR-fpr-fldA-araE*
18	MXA	pZE-*MAL-MutL-mutS-glmE-xylA*$_{CC}$	pZA-*Bamb_4925-4923-4922-4918-xylB-xylC-xylD-DR64_8450*	pZS-*gdhA-btuB-btuR-fpr-fldA-araE*

pZE plasmid backbone genotype: ColE1 origin, AmpR;
pZA plasmid backbone genotype: P15A origin, KanR;
pZS plasmid backbone genotype: pUC origin, SpecR.

(3.58 g/l) than no transporter strain 1 (3.47 g/l). From the time-course curves (Fig. S1 **A**–**D**) of the fermentation, we observed that XylFGH (strain 4) did not enhance D-xylose consumption and 8.7 g/l D-xylose was left at the end of the fermentation. Oppositely, XylE (strain 3) improved D-xylose transportation and 20 g/l of D-xylose was completely consumed after 36 h just as AraE did (strain 5). The final mesaconate titer of strain 3 reached 5.92 g/l..

The other three strains (strains 6, 7, and 8) were constructed for the L-arabinose pathway. The three strains were the MA1 strain transformed with plasmids pZA-*araC-araD-araA-araB*, pZE-*MAL-MutL-mutS-glmE-xylA*$_{CC}$, and the pZS plasmid containing the B12 regeneration pathway and different pentose transporters, respectively. Strain 6 overexpressed the symporter, AraE; strain 7 overexpressed the ABC transporter, AraFGH; strain 8 overexpressed the D-xylose symporter,

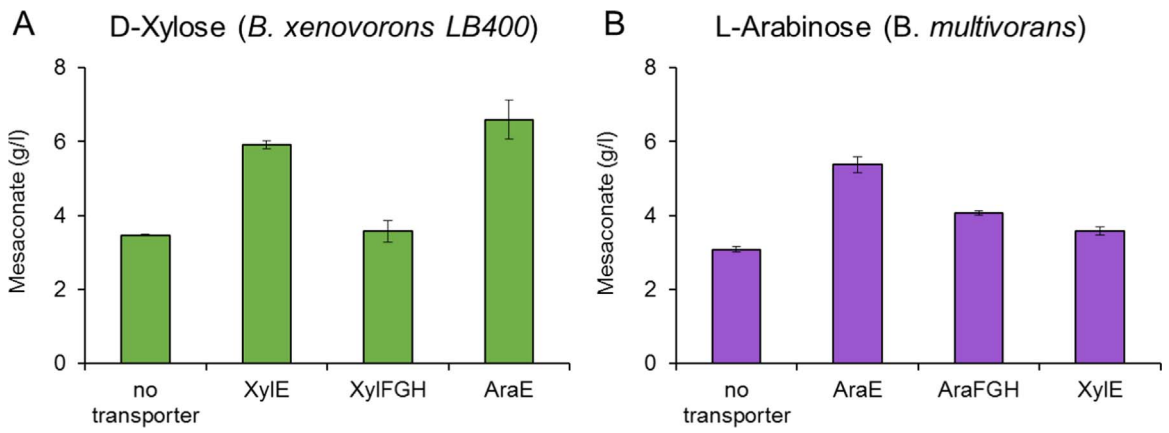

Fig. 2. Overexpression of pentose transporters to improve mesaconate production from D-xylose and L-arabinose. (A) Mesaconate production from D-xylose by strain 1 (no transporter), strain 3 (XylE), strain 4 (XylFGH), and strain 5 (AraE). XylE and AraE are proton symporters. XylFGH is a D-xylose specific ABC transporter. (B) Mesaconate production from L-arabinose by strain 2 (no transporter), strain 6 (AraE), strain 7 (AraFGH), and strain 8 (XylE). AraFGH is a L-arabinose specific ABC transporter. All error bars shown represent SD (n=3).

XylE. After 48 h of fermentation (Fig. 2**B**), strain 6 performed best among the three and resulted in 5.37 g/l mesaconate. Due to the promiscuity of XylE, strain 8 also enhanced L-arabinose uptake and improved the mesaconate production titer to 3.71 g/l from 3.08 g/l produced by strain 2 (no transporter). Based on the time-course profiles (Fig. S2 **A**–**D**), AraFGH only slightly improved the L-arabinose uptake rate (10.8 g/l of L-arabinose consumption by strain 7 compared to 9.3 g/l of L-arabinose consumption by strain 2 with no transporter) and the resulted mesaconate titer was only 4.05 g/l. Notably, although XylE (strain 8) did enhance L-arabinose transportation, it could not consume all the L-arabinose (3.6 g/l L-arabinose was left). For both D-xylose and L-arabinose, AraE was the most effective transporter for mesaconate production, and the ABC transporters (XylFGH and AraFGH) only slightly improved the pentose transportation in this study.

3.3. Screening operons of nonphosphrylative metabolism for mesaconate production

After we identified AraE as the most effective transporter for both D-xylose and L-arabinose, various operons of the nonphosphorylative metabolism were screened for optimal mesaconate production. For D-xylose pathway, three operons were tested for their activity towards mesaconate production. In the previous section, strain 5 which contained the *DR64_8447-8448-8449-8450* operon from *B. xenovorans LB400* was used to screen pentose transporters. For the other two operons, strain 9 contained the *xylB-xylC-xylD-xylX* operon from *Caulobacter crescentus*(Stephens et al., 2007) and strain 10 contained the *xylB-xylC-xylD-DR64_8250* operon which is a synthetic operon with the first three genes from *C. crescentus*(*xylB-xylC-xylD*) and the last gene (*DR64_8450*) from *B. xenovorans LB400*. We constructed this operon by combining the genes from two organisms since the enzyme KdxD from the *B. xenovorans LB400* operon was reported to have a higher in vitro activity (DR64_8250, k_{cat}/K_m=0.53 $s^{-1}mM^{-1}$) than that from the *C. crescentus* operon (XylX, k_{cat}/K_m=0.26 $s^{-1}mM^{-1}$) (Tai et al., 2016). On the other hand, *C. crescentus* operon has more active XDH and XD than the *B. xenovorans LB400* operon. When the three strains were subjected to fermentation, strain 10 with the synthetic operon was the best performing strain and produced 7.60 g/l mesaconate after 48 h (Fig. 3**A**)..

Three L-arabinose operons were also tested for mesaconate production via the nonphosphorylative metabolism. Strain 6 containing the

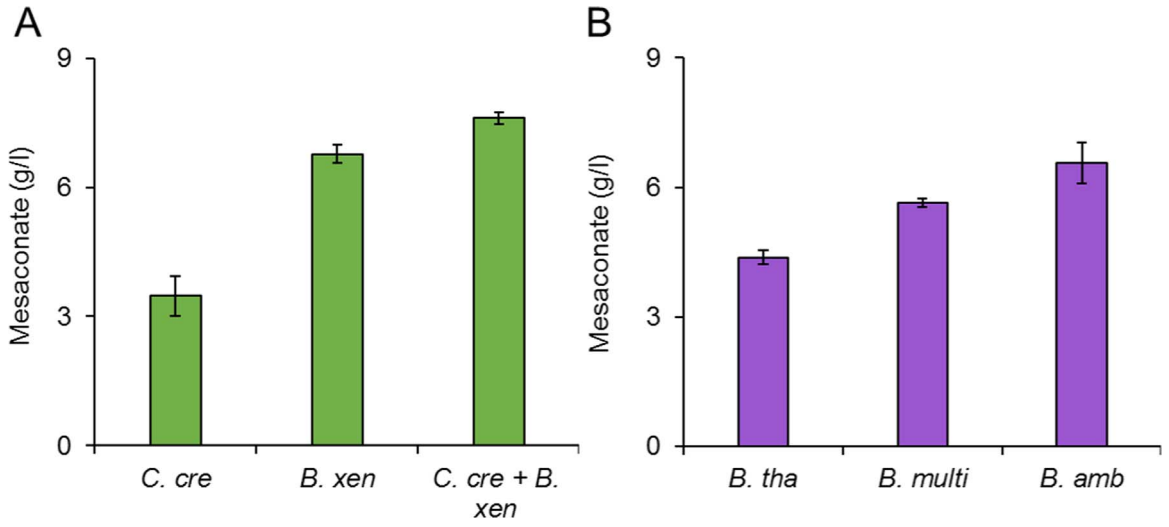

Fig. 3. Screening nonphosphorylative metabolism operons for mesaconate production from D-xylose and L-arabinose. All strains overexpressed AraE to enhance pentose transportation. (A) Three D-xylose operons were examined. Strain 9 contained the *C. cre* operon (*xylB-xylC-xylD-xylX*). Strain 5 contained the *B. xen*operon (*DR64_8447-8448-8449-8450*). Strain 10 contained the synthetic *C. cre + B. xen* operon (*xylB-xylC-xylD-DR64_8250*). (B) Three L-arabinose operons were examined. Strain 12 contained the *B. tha* operon (*BTH_II1632-1630-1629-1625*). Strain 6 contained the *B. multi* operon (*araC-araD-araA-araB*). Strain 11 contained the *B. amb* operon (*Bamb_4925-4923-4922-4918*). All error bars shown represent SD (n=3).

araC-araD-araA-araB operon from *B. multivorans*was used in the previous section. Strain 11 contained the *B. ambifaria* operon *Bamb_4925-4923-4922-4918* and strain 12 contained the *B. thailandensis* operon *BTH_II1632-1630–1629-1625*. Among the three strains, strain 11 with *B. ambifaria* operon enabled the highest mesaconate production at 6.55 g/l (Fig. 3**B**). *B. thailandensis* operon was the least active and only produced 4.38 g/l mesaconate (Fig. 3**B**).

3.4. Optimization of mesaconate biosynthesis by metabolic engineering

To further optimize mesaconate production from D-xylose and L-arabinose via this nonphosphorylative metabolism, we applied metabolic engineering strategies to drive the carbon flux towards the desired metabolite. *E. coli* gene *sucA* encodes a subunit of 2-KG decarboxylase (Buck et al., 1986) which catalyzes the conversion of 2-KG to succinyl-CoA in the TCA cycle and diverts the carbon flux from glutamate production. Therefore, we knocked out *sucA* gene in the production strains MX1 and MA1 to generate strains MX2 (MX1 Δ*sucA*) and MA2 (MA1 Δ*sucA*), respectively. On the other hand, *E. coli* gene *gdhA* encoding glutamate dehydrogenase (Sakamoto et al., 1975) which catalyzes the conversion of 2-KG into glutamate and can potentially enhance mesaconate production due to a larger glutamate pool. Therefore, the strategy was applied to optimize mesaconate production by cloning *gdhA* into the pZS plasmids to generate plasmid pZS-*gdhA-btuB-btuR-fpr-fldA-araE*.

Time-course profiles of the engineered strains were shown in Fig. 4. For the D-xylose pathway, strain 13 (MX2 host strain transformed with pZE-*MAL-MutL-mutS-glmE-xylA*$_{CC}$, pZA-*xylB-xylC-xylD-DR64_8450*, and pZS-*btuB-btuR-fpr-fldA-araE*) produced 10.59 g/l mesaconate (Fig. 4**B**). Compared to strain 10 (Fig. 4A), it enhanced mesaconate production by 34%. When *gdhA* was overexpressed in the pZS plasmid, strain 14 could further improve the mesaconate production to 12.53 g/l from 20 g/l D-xylose after 48 h (Fig. 4**C**). Similarly, *sucA* knockout (strain 15) improved mesaconate production from L-arabinose, from 6.00 g/l (Fig. 4**D**) to 11.50 g/l (Fig. 4**E**). Overexpression of *gdhA* (strain 16) further improved mesaconate titer to 13.25 g/l from 20 g/l L-arabinose (Fig. 4**F**). For the D-xylose pathway, the single *sucA* knockout strain could grow better than strain 11 due to less acetate production. OD_{600} of strain 13 kept increasing to OD_{600}=21.13 at the end of fermentation. Acetate production was only 2.22 g/l at 48 h. Similar trends were observed in the time-course profile of strain 15 for L-arabinose. There was less acetate production compared with strain 14 and only 0.90 g/l acetate was produced at the end of the fermentation. These results showed that mesaconate production could be increased from pentoses in lignocellulosic hydrolysates by modulating carbon flux and increasing glutamate pool from nonphosphorylative metabolism..

3.5. Mesaconateproduction by co-utilization of D-xylose, and L-arabinose

After we successfully engineered the nonphosphorylative metabolism to produce mesaconate from D-xylose and L-arabinose, the next step is to construct the strain that can utilize D-xylose and L-arabinose simultaneously for mesaconate production. When all glucose, D-xylose, and L-arabinose are provided in the culture medium, not only glucose will inhibit uptake of the pentoses, but also there is reciprocal regulation of L-arabinose and D-xylose metabolism (Koirala et al., 2016).. Since the nonphosphorylative metabolism is orthogonal to the intrinsic *E. coli* pentose metabolism, it may be a promising candidate that can be applied to overcome the CCR and reciprocal inhibition of pentose. To tackle this challenge, we constructed a plasmid (pZA-*Bamb_4925-4923-4922-4918-xylB-xylC-xylD-DR64_*

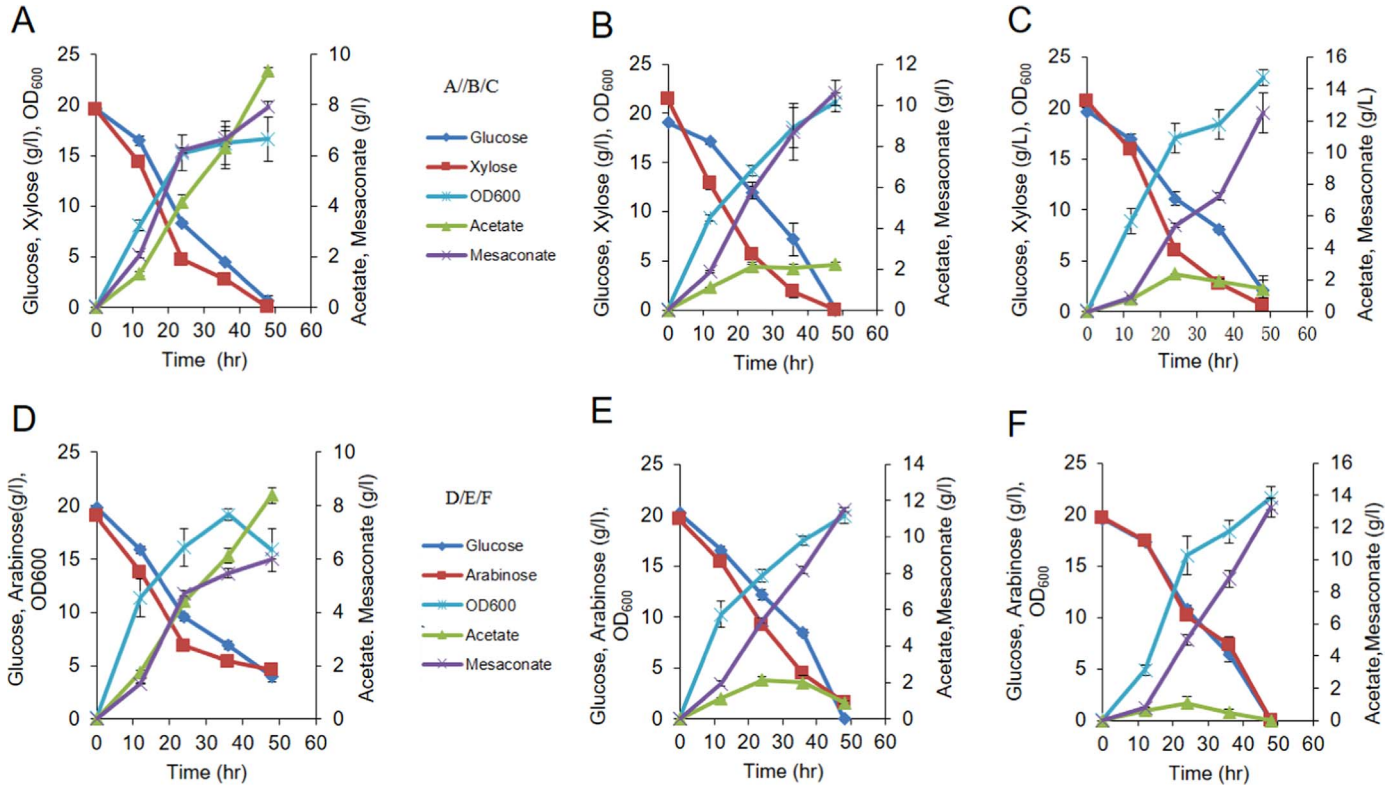

Fig. 4. Optimization of mesaconate production from D-xylose and L-arabinose via nonphosphorylative metabolism. (A) All three D-xylose strain were constructed based on the synthetic *C. cre* + *B. xen* operon and had AraE overexpressed to enhance pentose transportation. Strain 13 was based on *ΔsucA* strain and strain 14 was based on *ΔsucA* strain with *gdhA* overexpressed by the pZS plasmid. (B) All three L-arabinose strain were constructed based on the *B. amb* operon and had AraE overexpressed to enhance pentose transportation. Strain 15 was based on Δ*sucA* strain and strain 16 was based on *ΔsucA* strain with *gdhA* overexpressed by the pZS plasmid. (C) Time-course profile of strain 14. (D) Time-course profile of strain 16. Error bars are ± SD for n=3 independent experiments.

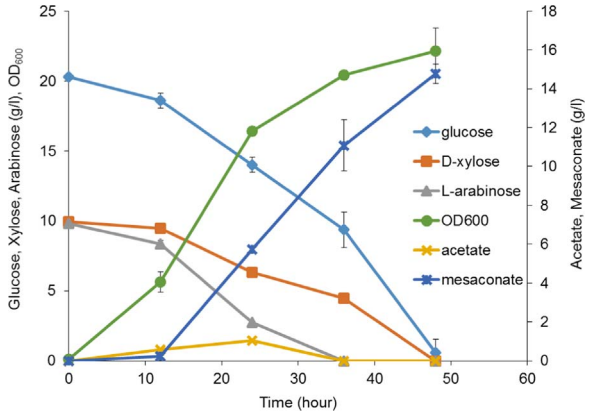

Fig. 5. Time-course profile of strain 17. The engineered strain co-utilized glucose, D-xylose, and L-arabinose for mesaconate production. Error bars are ± SD for n=3 independent fermentation experiments.

8450) that contained the synthetic D-xylose operon and the *B. ambifaria* L-arabinose operon due to their highest activities among the tested operons for D-xylose and L-arabinose consumption, respectively. AraE was chosen as the pentose transporter since it is promiscuous and is the most effective transporter for both D-xylose and L-arabinose as shown in previous sections. Strain MX2 was thus transformed with plasmids *pZE-MAL-MutL-mutS-glmE-xylA$_{CC}$*, pZA-*Bamb_4925-4923-4922-4918-xylB-xylC-xylD-DR64_8450*, and *pZS-btuB-btuR-fpr-fldA-araE* to generate strain 17. During fermentation, 20 g/l glucose was supplemented for cell growth, and 10 g/l D-xylose and 10 g/l L-arabinose were fed for mesaconate production. The engineered strain 17 utilized three sugars simultaneously and produced 14.75 g/l mesaconate after 48 h (Fig. 5). From the time curve (Fig. 5), we can see that although L-arabinose was consumed with a faster rate than D-xylose and was completely consumed after 36 h, the engineered strain could use all three sugars simultaneously was able to use all D-xylose after 48 h. The yield of mesaconate was 0.74 g/g of combined D-xylose and L-arabinose which accounts for 85% of the theoretical yield (0.87 g/g)..

In order to investigate mesaconateproduction from D-glucose, D-xylose and L-arabinose, the *icd* gene in strains MXA was not deleted. Strain MXA was thus transformed with plasmids *pZE-MAL-MutL-mutS-glmE-xylA$_{CC}$*, pZA-*Bamb_4925-4923-4922-4918-xylB-xylC-xylD-DR64_8450*, and *pZS-btuB-btuR-fpr-fldA-araE* to generate strain 18. During fermentation, 20 g/l glucose was supplemented for cell growth and mesaconate production, and 10 g/l D-xylose and 10 g/l L-arabinose were fed for mesaconate production. However, the engineered strain 18 could only produce 7.6 g/L mesaconate because it could not consume all of pentoses (6.1 g/L D-xylose and 2.2 g/L L-arabinose were left, respectively) (Fig S3). The current strain requires more engineering efforts in the future to enable simultaneous consumption of all sugars.

4. Conclusion

Successful conversion of D-xylose and L-arabinose, important sugars in hemicellulose, to a branched unsaturated dicarboxylic acid mesaconate via efficient nonphosphorylative metabolism was demonstrated. To alleviate CCR in a mixture of glucose and pentose (D-xylose or L-arabinose), various pentose transporters were overexpressed and tested. We identified that AraE, a proton symporter, was the most effective transporter for both D-xylose and L-arabinose. Three D-xylose operons and three L-arabinose operons were screened for mesaconate production. The synthetic D-xylose operon (*xylB-xylC-xylD-DR64_8250*) created by combining the first three genes (encode XDH, XL, and XD) from *C. crescentus* and the last gene from *B. xenovorans LB400* (encodes KdxD) enabled the highest mesaconate production titer from D-xylose. The *B. ambifaria* operon (*Bamb_4925-4923-4922-4918*) was the most active operon for L-arabinose. To further optimize mesaconate production, we applied metabolic engineering strategies by knocking out competing pathway gene *sucA* and overexpressing *gdhA* which encodes glutamate dehydrogenase to enlarge the glutamate pool. Mesaconate production was successfully improved from 7.60 to 12.53 g/l from 20 g/l of D-xylose after implementing these two modifications. Similarly, mesaconate production titers were increased from 6.55 to 13.24 g/l from 20 g/l L-arabinose. Finally, the two best-performing D-xylose and L-arabinose operons were integrated into a single strain. Therefore, the engineered strain can simultaneously utilize D-xylose and L-arabinose for mesaconate production. By supplementing 10 g/l of D-xylose and 10 g/l of L-arabinose, strain 17 overexpressing the two operons was able to produce mesaconate at 14.75 g/l with a yield of 0.74 g/g of pentoses. Herein, we demonstrated a novel, efficient, and high-yield biosynthetic platform to produce mesaconate in *E. coli* from biomass pentoses.

Acknowledgements

This work was supported by the National Science Foundation (NSF) under research Grant BBE-1604728 and the Center for Sustainable Polymers CHE-1413862.

Competing financial interest statement

The authors declare no competing financial interests.

Appendix A. Supplementary material

Supplementary data associated with this article can be found in the online version at doi:10.1016/j.ymben.2016.09.007.

References

Adom, F., Dunn, J.B., Han, J., Sather, N., 2014. Life-cycle fossil energy consumption and greenhouse gas emissions of bioderived chemicals and their conventional counterparts. Environ. Sci. Technol. 48, 14624–14631.
Baba, T., Ara, T., Hasegawa, M., Takai, Y., Okumura, Y., Baba, M., Datsenko, K.A., Tomita, M., Wanner, B.L., Mori, H., 2006. Construction of Escherichia coli K-12 in-frame, single-gene knockout mutants: the Keio collection. Mol. Syst. Biol. 2, 0008.
Bechthold, I., Bretz, K., Kabasci, S., Kopitzky, R., Springer, A., 2008. Succinic acid: a new platform chemical for biobased polymers from renewable resources. Chem. Eng. Technol. 31, 647–654.
Blair, A.H., Barker, H.A., 1966. Assay and purification of (+) -citramalate hydro-lyase components from Clostridium tetanomorphum. J. Biol. Chem. 241, 400–408.
Brouns, S.J., Walther, J., Snijders, A.P., van de Werken, H.J., Willemen, H.L., Worm, P., de Vos, M.G., Andersson, A., Lundgren, M., Mazon, H.F., van den Heuvel, R.H., Nilsson, P., Salmon, L., de Vos, W.M., Wright, P.C., Bernander, R., van der Oost, J., 2006. Identification of the missing links in prokaryotic pentose oxidation pathways: evidence for enzyme recruitment. J. Biol. Chem. 281, 27378–27388.
Buck, D., Spencer, M.E., Guest, J.R., 1986. Cloning and expression of the cuccinyl-Coa synthetase genes of Escherichia coli K12. J. Gen. Microbiol. 132, 1753–1762.
Buckel, W., Barker, H.A., 1974. Two pathways of glutamate fermentation by anaerobic bacteria. J. Bacteriol. 117, 1248–1260.
Cirino, P.C., Chin, J.W., Ingram, L.O., 2006. Engineering Escherichia coli for xylitol production from glucose-xylose mixtures. Biotechnol. Bioeng. 95, 1167–1176.
Daruwalla, K.R., Paxton, A.T., Henderson, P.J., 1981. Energization of the transport systems for arabinose and comparison with galactose transport in Escherichia coli. Biochem J. 200, 611–627.
Desai, T.A., Rao, C.V., 2010. Regulation of arabinose and xylose metabolism in Escherichia coli. Appl Environ. Microbiol. 76, 1524–1532.
Dien, B.S., Nichols, N.N., Bothast, R.J., 2002. Fermentation of sugar mixtures using Escherichia coli catabolite repression mutants engineered for production of L-lactic acid. J. Ind. Microbiol. Biotechnol. 29, 221–227.
Feldmann, S.D., Sahm, H., Sprenger, G.A., 1992. Cloning and expression of the genes for xylose isomerase and xylulokinase from Klebsiella pneumoniae 1033 in Escherichia coli K12. Mol. Gen. Genet. 234, 201–210.
Gillham, H.C.Sherr, A.E., 1969. Flame-retardant Agents for Thermoplastic Products. U.S. Patent US3431324A.
Goerke, B., Stulke, J., 2008. Carbon catabolite repression in bacteria: many ways to make the most out of nutrients. Nat. Rev. Microbiol. 6, 613–624.
Guccione, E., Hitchcock, A., Hall, S.J., Mulholland, F., Shearer, N., van Vliet, A.H.M., Kelly, D.J., 2010. Reduction of fumarate, mesaconate and crotonate by Mfr, a novel oxygen-regulated periplasmic reductase in Campylobacter jejuni. Environ. Microbiol.

12, 576–591.
Hasona, A., Kim, Y., Healy, F.G., Ingram, L.O., Shanmugam, K.T., 2004. Pyruvate formate lyase and acetate kinase are essential for anaerobic growth of Escherichia coli on xylose. J. Bacteriol. 186, 7593–7600.
Hong, U.G., Park, H.W., Lee, J., Hwang, S., Kwak, J., Yi, J., Song, I.K., 2013. Hydrogenation of succinic acid to 1,4-butanediol over rhenium catalyst supported on copper-containing mesoporous carbon. J. Nanosci. Nanotechnol. 13, 7448–7453.
Jarmander, J., Hallstrom, B.M., Larsson, G., 2014. Simultaneous uptake of lignocellulose-based monosaccharides by Escherichia coli. Biotechnol. Bioeng. 111, 1108–1115.
Jojima, T., Omumasaba, C.A., Inui, M., Yukawa, H., 2010. Sugar transporters in efficient utilization of mixed sugar substrates: current knowledge and outlook. Appl Microbiol Biotechnol. 85, 471–480.
Koirala, S., Wang, X., Rao, C.V., 2016. Reciprocal regulation of L-Arabinose and D-Xylose metabolism in Escherichia coli. J. Bacteriol. 198, 386–393.
Kronen, M., Sasikaran, J., Berg, I.A., 2015. Mesaconase activity of class I fumarase contributes to mesaconate utilization by Burkholderia xenovorans. Appl Environ. Microbiol 81, 5632–5638.
Lopez-Garzon, C.S., Straathof, A.J.J., 2014. Recovery of carboxylic acids produced by fermentation. Biotechnol. Adv. 32, 873–904.
Miller, J.H., 1972. Experiments in Molecular Genetics. Cold Spring Harbor Laboratory, New York.
Sakamoto, N., Kotre, A.M., Savageau, M.A., 1975. Glutamate dehydrogenase from Escherichia coli: purification and properties. J. Bacteriol. 124, 775–783.
Sato, K., Aoki, M., Noyori, R., 1998. A "Green" route to adipic acid: direct oxidation of cyclohexenes with 30% hydrogen peroxide. Science 281, 1646–1647.
Shamanna, D.K., Sanderson, K.E., 1979. Uptake and catabolism of D-xylose in Salmonella typhimurium LT2. J. Bacteriol. 139, 64–70.
Song, S.G., Park, C., 1998. Utilization of D-ribose through D-xylose transporter. Fems Microbiol. Lett. 163, 255–261.
Sonntag, F., Buchhaupt, M., Schrader, J., 2014. Thioesterases for ethylmalonyl-CoA pathway derived dicarboxylic acid production in Methylobacterium extorquens AM1. Appl. Microbiol. Biotechnol. 98, 4533–4544.
Sonntag, F., Muller, J.E.N., Kiefer, P., Vorholt, J.A., Schrader, J., Buchhaupt, M., 2015. High-level production of ethylmalonyl-CoA pathway-derived dicarboxylic acids by Methylobacterium extorquens under cobalt-deficient conditions and by polyhydroxybutyrate negative strains. Appl. Microbiol. Biotechnol. 99, 3407–3419.
Stephens, C., Christen, B., Fuchs, T., Sundaram, V., Watanabe, K., Jenal, U., 2007. Genetic analysis of a novel pathway for D-xylose metabolism in Caulobacter crescentus. J. Bacteriol. 189, 2181–2185.
Stulke, J., Hillen, W., 1999. Carbon catabolite repression in bacteria. Curr. Opin. Microbiol. 2, 195–201.
Tai, Y.-S., Xiong, M., Jambunathan, P., Wang, J., Wang, J., Stapleton, C., Zhang, K., 2016. Engineering nonphosphorylative metabolism to generate lignocellulose-derived products. Nat. Chem. Biol. 12, 247–253.
Uzum, O.B., Karadag, E., 2005. Equilibrium swelling studies of highly swollen acrylamide/mesaconic acid hydrogels. J. Appl. Polym. Sci. 96, 2253–2259.
Wang, J., Zhang, K., 2015. Production of mesaconate in Escherichia coli by engineered glutamate mutase pathway. Metab. Eng. 30, 190–196.
Weber, C., Farwick, A., Benisch, F., Brat, D., Dietz, H., Subtil, T., Boles, E., 2010. Trends and challenges in the microbial production of lignocellulosic bioalcohol fuels. Appl. Microbiol. Biotechnol. 87, 1303–1315.
Weimberg, R., 1961. Pentose oxidation by Pseudomonas fragi. J. Biol. Chem. 236, 629–635.
White, J.D., Sheldon, B.G., 1981. Intramolecular Diels-Alder reactions of sorbyl citraconate and mesaconate esters. J. Org. Chem. 46, 2273–2280.